



Contents lists available at ScienceDirect

Ain Shams Engineering Journal

journal homepage: www.sciencedirect.com



Electrical Engineering

## DSTATCOM deploying CGBP based $\text{icos } \phi$ neural network technique for power conditioning

Mrutyunjaya Mangaraj\*, Anup Kumar Panda

Department of Electrical Engineering, National Institute of Technology, Rourkela 769008, India

### ARTICLE INFO

#### Article history:

Received 24 August 2016

Accepted 13 November 2016

Available online xxxxx

#### Keywords:

CGBP based  $\text{icos } \phi$  neural network

DSTATCOM

MATLAB

RTDS

### ABSTRACT

Present investigation focuses design & simulation study of a three phase three wire DSTATCOM deploying a conjugate gradient back propagation (CGBP) based  $\text{icos } \phi$  neural network technique. It is used for various tasks such as source current harmonic reduction, load balancing and power factor correction under various loading which further reduces the DC link voltage of the inverter. The proposed technique is implemented by mathematical analysis with suitable learning rate and updating weight using MATLAB/Simulink. It predicts the computation of fundamental weighting factor of active and reactive component of the load current for the generation of reference source current smoothly. Its design capability is reflected under to prove the effectiveness of the DSTATCOM. The simulation waveforms are presented and verified using both MATLAB & real-time digital simulator (RTDS). It shows the better performance and maintains the power quality norm as per IEEE-519 by keeping THD of source current well below 5%.

© 2016 Ain Shams University. Production and hosting by Elsevier B.V. This is an open access article under the CC BY-NC-ND license (<http://creativecommons.org/licenses/by-nc-nd/4.0/>).

### 1. Introduction

In recent years, various loads such as industrial, commercial and domestic industrial loads are the integral part of the modern electrical distribution system. These are like personal computers, uninterruptible power supplies (UPS), inverters, fax machines, printers, fluorescents lighting, variable speed drives, induction heating and electric tractions etc. Basically, these loads are the main reason in reducing the power quality performances. So that whole system suffers from the various problems like reactive power burden, harmonics contents, poor voltage regulation and load unbalancing and so on which raises more loss in the feeder, transformers, generators and shrinks active power flow. Also it reduces the efficiency and life span of the equipment [1]. The other reason is that less cost of custom power devices (CPDS) to sustain the market demands. In view of these two reasons, most of the research is being heartened by manufacturing industries. There are several types of CPDs are used in the distribution system for specific purpose. DSTATCOM is one of CPDs. This is used for various purposes like reactive power compensation, harmonic reduction, power factor correction and load balancing etc. [2]. The extent of accuracy of DSTATCOM is

much dependent on the design and modelling of control mechanism for computation of reference current [3–13]. To serve this purpose, many algorithms like synchronous reference frame (SRF) theory [3–5], Lyapunov-function based control theory [6], instantaneous reactive power (IRP) theory [7,8], synchronous detection (SD) theory [9], fryze power theory [10],  $\text{icos } \phi$  control technique [11,12] are adopted.

Besides these, generation of switching signal and reference current estimation of voltage source converter (VSC), many soft computing training based algorithms have been adopted like neural network (NN) and adaptive neuro-fuzzy inference system (ANFIS) [13–17]. Among these, NN is more popular in the distribution system due to the following advantages such as dynamic operation, self-organization and fault reduction through adaptive learning. Apart from them, many other control algorithms such as the recurrent Neural Network [18,19], Zhang NN [20], bi-Projection NN [21] can also be used for the control of d-FACTS devices.

Apart from them, there are other various types of neural network such as gradient descent back propagation (GDBP), GDBP with momentum (GDBPM), variable learning rate GDBPM (VLGDBPM), CGBP and quasi Newton back propagation (QNBP). The advantage of CGBP algorithm relies on adjustment of the weights along conjugate directions rather than steepest descent direction which reduces the step size and performance function as well [22]. In view of certain modification of control technique, CGBP is combined with conventional  $\text{icos } \phi$  control technique in

Peer review under responsibility of Ain Shams University.

\* Corresponding author.

E-mail addresses: [mmangaraj.ee@gmail.com](mailto:mmangaraj.ee@gmail.com) (M. Mangaraj), [akpanda.ee@gmail.com](mailto:akpanda.ee@gmail.com) (A.K. Panda).<http://dx.doi.org/10.1016/j.asej.2016.11.009>

2090–4479/© 2016 Ain Shams University. Production and hosting by Elsevier B.V.

This is an open access article under the CC BY-NC-ND license (<http://creativecommons.org/licenses/by-nc-nd/4.0/>).

Please cite this article in press as: Mangaraj M, Panda AK. DSTATCOM deploying CGBP based  $\text{icos } \phi$  neural network technique for power conditioning. Ain Shams Eng J (2016), <http://dx.doi.org/10.1016/j.asej.2016.11.009>

this paper. This attempt is taken for the following purposes such as source current harmonic reduction, load balancing and power factor correction etc. and also reduced rating of DSTATCOM is obtained. So CGBP algorithm is also feasible solution to show the better performance in driving DSTATCOM under various loading operating conditions.

**2. DSTATCOM with power distribution system**

The schematic diagram of DSTATCOM with power distribution system is depicted in the Fig. 1. Here, the DSTATCOM is configured for three phase three wire (3P3W) system as 3P3W balanced source supplied to 3P3W nonlinear load. The detail CGBP based  $\text{icos } \phi$  control mechanism is depicted in Fig. 2 and CGBP based  $\text{icos } \phi$  control architecture is shown in Fig. 3. The systematic procedure for the estimation of switching signal generation is described as follows.

**2.1. Calculation of weighted value of fundamental active and reactive components**

The weighted values of the active components of the load currents ( $i_{lap}$ ,  $i_{lbp}$  &  $i_{lcp}$ ) are expressed as

$$\begin{bmatrix} i_{lap} \\ i_{lbp} \\ i_{lcp} \end{bmatrix} = w_0 + [i_{la} \cos \phi_{la} \quad i_{lb} \cos \phi_{lb} \quad i_{lc} \cos \phi_{lc}] \begin{bmatrix} u_{ap} \\ u_{bp} \\ u_{cp} \end{bmatrix} \quad (1)$$

where  $w_0$  is the initial weight, and  $i_{la}$ ,  $i_{lb}$  and  $i_{lc}$  are the three phase load currents,  $u_{ap}$ ,  $u_{bp}$  and  $u_{cp}$  are the in-phase unit voltages.

These in-phase unit voltages at point of common coupling (PCC) are obtained from the following equations

$$\begin{bmatrix} u_{ap} \\ u_{bp} \\ u_{cp} \end{bmatrix} = \frac{1}{v_t} \begin{bmatrix} v_{sa} \\ v_{sb} \\ v_{sc} \end{bmatrix} \quad (2)$$

where  $v_{sa}$ ,  $v_{sb}$  and  $v_{sc}$  are phase voltage correspond to a, b and c-phase respectively and the sensed PCC voltages ( $v_t$ ) is calculated as

$$v_t = \sqrt{\frac{2(v_{sa}^2 + v_{sb}^2 + v_{sc}^2)}{3}} \quad (3)$$

The above extracted three phase currents of  $i_{lap}$ ,  $i_{lbp}$  and  $i_{lcp}$  are passed through the continuous sigmoid function. The output signals  $Z_{ap}$ ,  $Z_{bp}$  and  $Z_{cp}$  can be obtained by the following equations

$$\begin{bmatrix} Z_{ap} \\ Z_{bp} \\ Z_{cp} \end{bmatrix} = \begin{bmatrix} f(i_{lap}) \\ f(i_{lbp}) \\ f(i_{lcp}) \end{bmatrix} = 1 \div \begin{bmatrix} 1 + e^{-i_{lap}} \\ 1 + e^{-i_{lbp}} \\ 1 + e^{-i_{lcp}} \end{bmatrix} \quad (4)$$

The  $Z_{ap}$ ,  $Z_{bp}$  and  $Z_{cp}$  act as input signal which are processed through the hidden layer. These fundamental components are the output of this layer  $i_{ap1}$ ,  $i_{bp1}$  and  $i_{cp1}$  before processed through the sigmoid function are expressed as

$$\begin{bmatrix} i_{ap1} \\ i_{bp1} \\ i_{cp1} \end{bmatrix} = w_{01} + [w_{ap} \quad w_{bp} \quad w_{cp}] \begin{bmatrix} Z_{ap} \\ Z_{bp} \\ Z_{cp} \end{bmatrix} \quad (5)$$

where  $w_{01}$  is the initial weight of the hidden layer,  $w_{ap}$ ,  $w_{bp}$  and  $w_{cp}$  are three updated weighted values of active component of load currents.

The updated weight ' $w_{ap1}$ ' of active component of a-phase load current can be expressed as

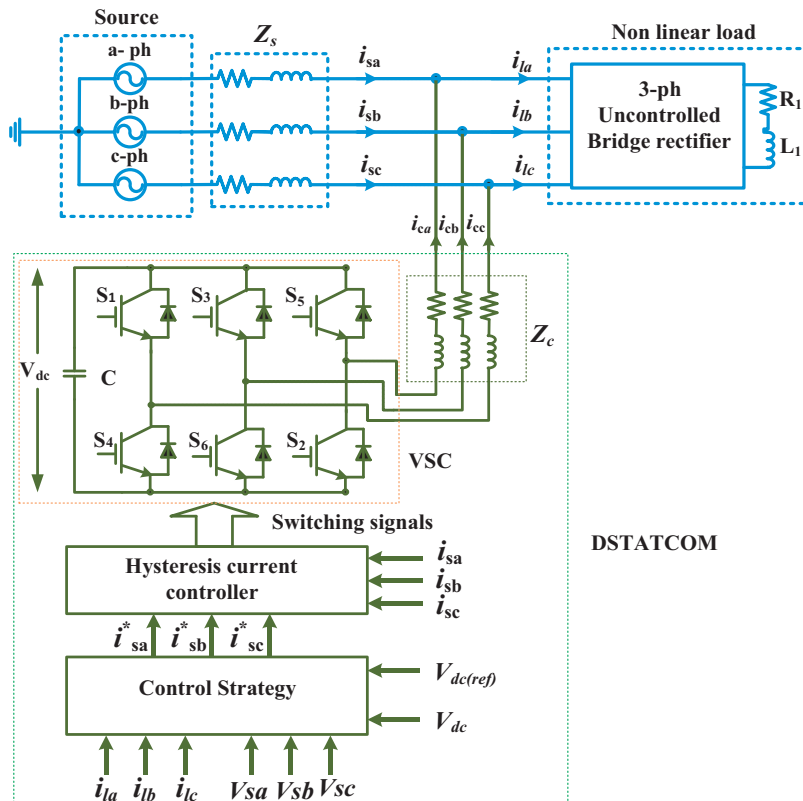


Figure 1. Schematic diagram of DSTATCOM with power distribution system.

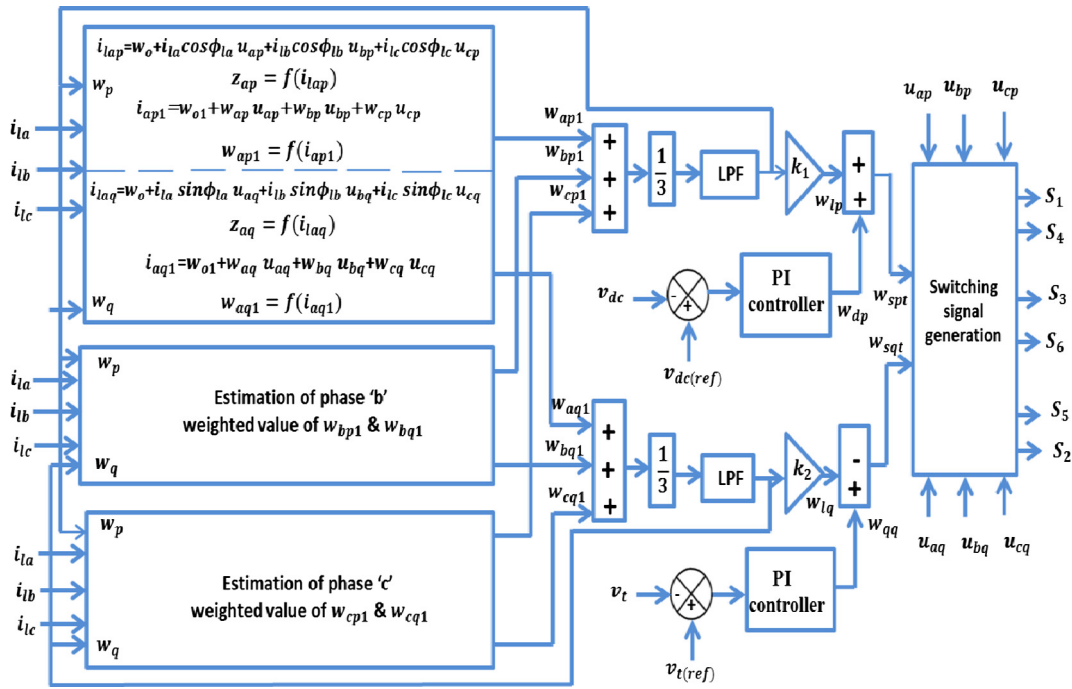


Figure 2. Block diagram for switching signals generation of VSC using CGBP based icos  $\phi$  control mechanism.

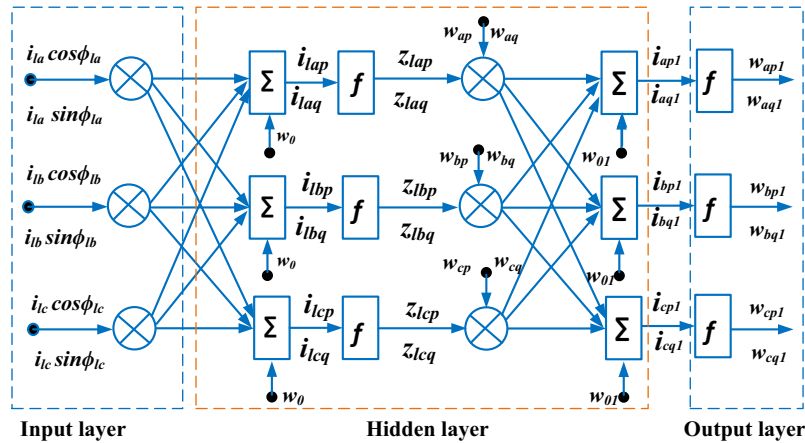


Figure 3. CGBP based icos  $\phi$  control architecture.

$$\begin{bmatrix} W_{ap} \\ W_{bp} \\ W_{cp} \end{bmatrix} = W_p + \mu_{p+1} [W_p - W_{ap1} \quad W_p - W_{bp1} \quad W_p - W_{cp1}] \begin{bmatrix} K_{ap} \\ K_{bp} \\ K_{cp} \end{bmatrix} \begin{bmatrix} f'(i_{ap1}) \\ f'(i_{bp1}) \\ f'(i_{cp1}) \end{bmatrix} \quad (6)$$

where  $K_{ap} = -f'(i_{ap1}) + B_{ap}Z_{ap(n-1)}$ .

$$B_{ap} = \frac{\Delta f'(i_{ap1})_{n-1}^T f'(i_{ap1})_n}{f'(i_{ap1})_{n-1}^T f'(i_{ap1})_{n-1}}$$

$$\Delta f'(i_{ap1})_{n-1}^T = f'(i_{ap1})_n^T - f'(i_{ap1})_{n-1}^T$$

where  $w_{ap1}$  is the a-phase fundamental weighted value of the active component of the load current, superscript ‘T’ is used for transpose,  $w_p$  is the average weighted value of the active component of load currents,  $\mu$  is the rate of learning,  $f'(i_{ap1})$  is the first derivative of  $i_{ap1}$  component and  $Z_{ap}$  is the output of the feedforward section of the hidden layer, etc.

The fundamental values  $i_{ap1}$ ,  $i_{bp1}$  and  $i_{cp1}$  are extracted using Fourier principle which processed through the sigmoid function act as an activation function can be calculated in terms of  $w_{ap1}$ ,  $w_{bp1}$  &  $w_{cp1}$  as

$$\begin{bmatrix} W_{ap1} \\ W_{bp1} \\ W_{cp1} \end{bmatrix} = \begin{bmatrix} f(i_{ap1}) \\ f(i_{bp1}) \\ f(i_{cp1}) \end{bmatrix} = 1 \div \begin{bmatrix} 1 + e^{-i_{ap1}} \\ 1 + e^{-i_{bp1}} \\ 1 + e^{-i_{cp1}} \end{bmatrix} \quad (7)$$

The average weighted value of active component of load current can be calculated as

$$w_p = \frac{W_{ap1} + W_{bp1} + W_{cp1}}{3} \quad (8)$$

The necessity of first order low-pass filters (LPF) is to extract the lower order components and then reduced by a scaled factor ‘ $k_1$ ’ to get the actual value  $w_{lp}$  in the control mechanism which is shown in Fig. 2.

In similar way, the weighted values of the reactive components of the load currents ( $i_{laq}$ ,  $i_{lbq}$  &  $i_{lcq}$ ) are expressed as

$$\begin{bmatrix} i_{laq} \\ i_{lbq} \\ i_{lcq} \end{bmatrix} = w_0 + [i_{la} \sin \phi_{la} \quad i_{lb} \sin \phi_{lb} \quad i_{lc} \sin \phi_{lc}] \begin{bmatrix} u_{aq} \\ u_{bq} \\ u_{cq} \end{bmatrix} \quad (9)$$

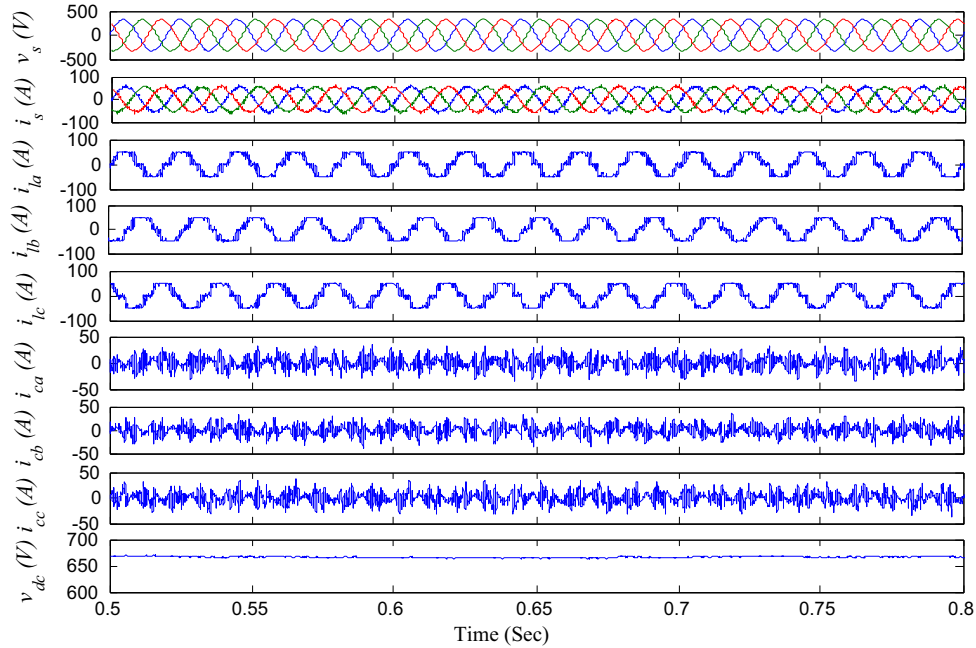
where  $u_{aq}$ ,  $u_{bq}$  &  $u_{cq}$  are the quadrature unit voltages correspond to a, b and c-phase respectively and can be expressed as

$$\begin{bmatrix} u_{aq} \\ u_{bq} \\ u_{cq} \end{bmatrix} = \frac{1}{\sqrt{3}} \begin{bmatrix} 0 & u_{bp} & u_{cp} \\ 3u_{ap} & u_{bp} & -u_{cp} \\ -3u_{ap} & 3u_{bp} & -u_{cp} \end{bmatrix} \quad (10)$$

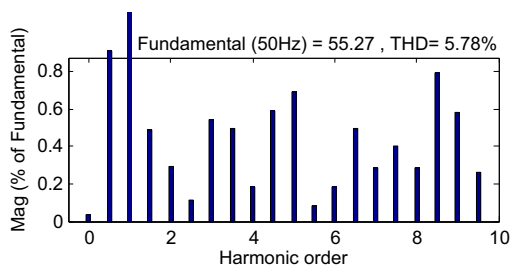
The above weighted values of  $i_{laq}$ ,  $i_{lbq}$  &  $i_{lcq}$  are passed through the sigmoid function for the estimation of three weighted values of reactive component of load currents ( $Z_{aq}$ ,  $Z_{bq}$  &  $Z_{cq}$ ) which can be expressed by the following equations

$$\begin{bmatrix} Z_{aq} \\ Z_{bq} \\ Z_{cq} \end{bmatrix} = \begin{bmatrix} f(i_{laq}) \\ f(i_{lbq}) \\ f(i_{lcq}) \end{bmatrix} = 1 \div \begin{bmatrix} 1 + e^{-i_{laq}} \\ 1 + e^{-i_{lbq}} \\ 1 + e^{-i_{lcq}} \end{bmatrix} \quad (11)$$

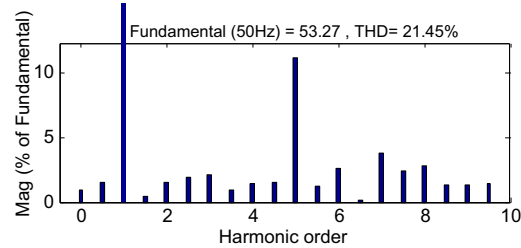
The estimated values of  $Z_{aq}$ ,  $Z_{bq}$  &  $Z_{cq}$  act as input signals are processed through the hidden layer. The three phase fundamental output components of this layer  $i_{aq1}$ ,  $i_{bq1}$  &  $i_{cq1}$  before processed through the sigmoid function are calculated as



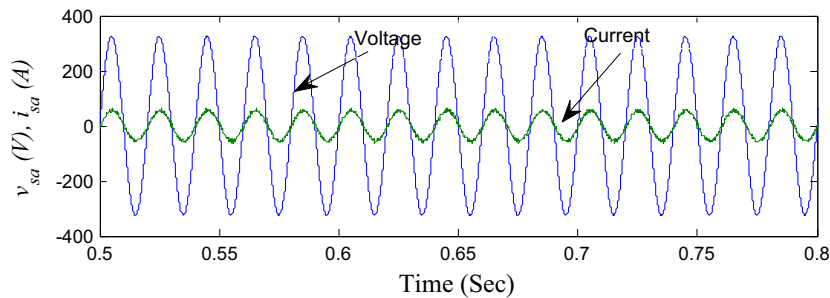
(i)



(ii)



(iii)



(iv)

**Figure 4.** (i) DSTATCOM under constant loading, (ii) Harmonics spectrum of source current, (iii) Harmonics spectrum of load current and (iv) a-phase source voltage and source current waveform.

$$\begin{bmatrix} i_{aq1} \\ i_{bq1} \\ i_{cq1} \end{bmatrix} = w_{01} + [w_{aq} \quad w_{bq} \quad w_{cq}] \begin{bmatrix} Z_{aq} \\ Z_{bq} \\ Z_{cq} \end{bmatrix} \quad (12)$$

$$\begin{bmatrix} W_{aq} \\ W_{bq} \\ W_{cq} \end{bmatrix} = W_q + \mu_{q+1} [W_q - W_{aq1} \quad W_q - W_{bq1} \quad W_q - W_{cq1}] \quad \begin{bmatrix} K_{aq} \\ K_{bq} \\ K_{cq} \end{bmatrix} \begin{bmatrix} f'(i_{aq1}) \\ f'(i_{bq1}) \\ f'(i_{cq1}) \end{bmatrix} \quad (13)$$

Here  $w_{aq}$ ,  $w_{bq}$  and  $w_{cq}$  are three updated weighted values of reactive component of currents.

The updated weight 'w<sub>aq1</sub>' of reactive component of a-phase load current can be expressed as

where  $K_{aq} = -f'(i_{aq1}) + B_{aq}Z_{aq(n-1)}$ .

$$B_{aq} = \frac{\Delta f'(i_{aq1})_{n-1}^T f'(i_{aq1})_n}{f'(i_{aq1})_{n-1}^T f'(i_{aq1})_{n-1}}$$

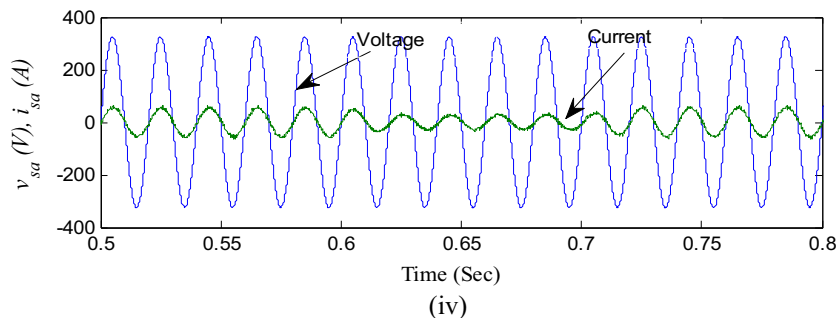
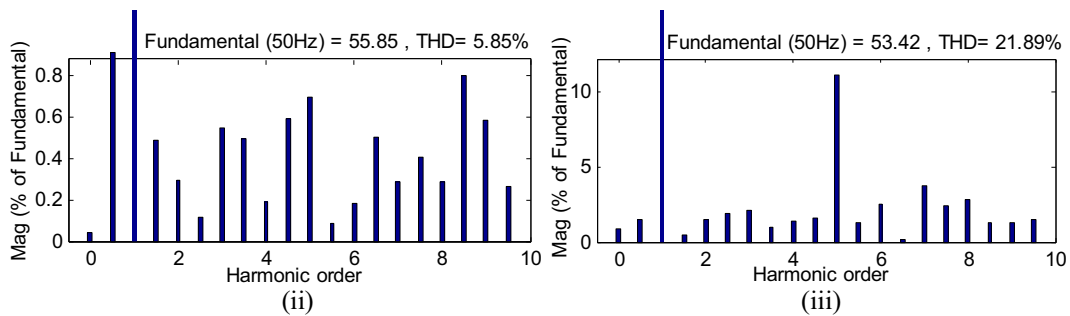
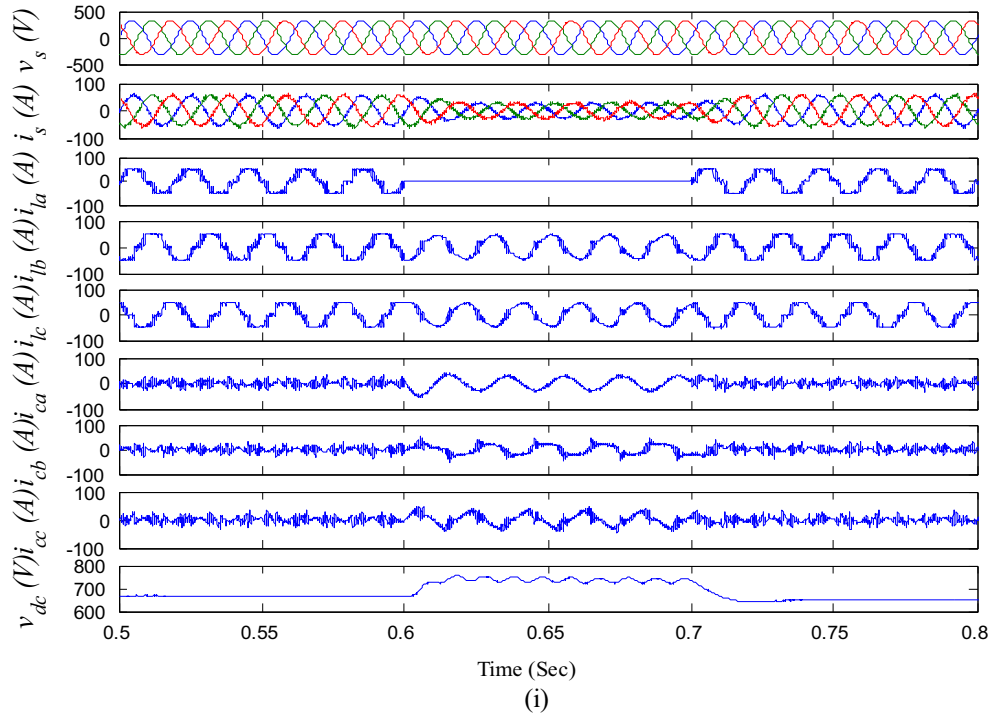


**Figure 5.** (i) DSTATCOM under variable loading, (ii) Harmonics spectrum of source current, (iii) Harmonics spectrum of load current and (iv) a-phase source voltage and source current waveform.

$$\Delta f'(i_{aq1})_{n-1}^T = f'(i_{aq1})_n^T - f'(i_{aq1})_{n-1}^T$$

where  $w_{aq1}$  is the a-phase fundamental weighted value of the reactive component of load current,  $w_q$  is the average weighted value of the reactive load current component,  $f'(i_{aq1})$  is the first derivative of  $i_{aq1}$  component and  $Z_{aq}$  is the output of the feedforward section of hidden layer, etc.

The fundamental values  $i_{aq1}$ ,  $i_{bq1}$  &  $i_{cq1}$  are extracted using Fourier principle which processed through the sigmoid function act as an activation function can be expressed in terms of  $w_{aq1}$ ,  $w_{bq1}$  and  $w_{cq1}$  as

$$\begin{bmatrix} w_{aq1} \\ w_{bq1} \\ w_{cq1} \end{bmatrix} = \begin{bmatrix} f(i_{aq1}) \\ f(i_{bq1}) \\ f(i_{cq1}) \end{bmatrix} = 1 \div \begin{bmatrix} 1 + e^{-i_{aq1}} \\ 1 + e^{-i_{bq1}} \\ 1 + e^{-i_{cq1}} \end{bmatrix} \quad (14)$$

The average weighted value of the reactive component of load current can be calculated as

$$w_q = \frac{w_{aq1} + w_{bq1} + w_{cq1}}{3} \quad (15)$$

The necessity of first order LPF is to extract the lower order components and then reduced by a scaled factor ' $k_2$ ' to get the actual value  $w_{lq}$  in the control mechanism which is shown in Fig. 2.

### 2.2. Computation of active component of reference source currents

The difference between reference dc voltage ' $v_{dc(ref)}$ ' and sensed dc voltage ' $v_{dc}$ ' is the error in dc voltage ( $v_{de}$ ) can be expressed as

$$v_{de} = v_{dc(ref)} - v_{dc} \quad (16)$$

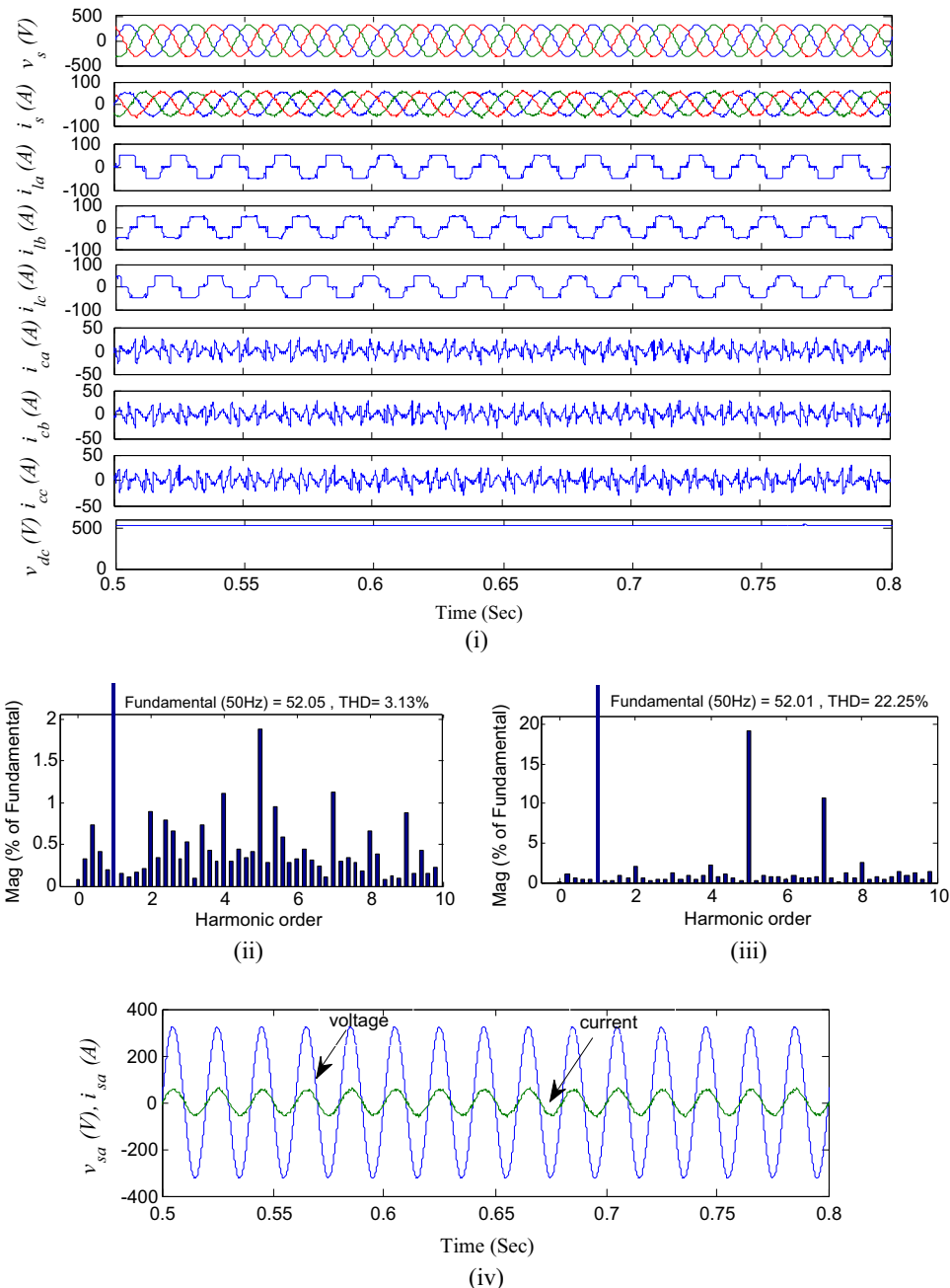


Figure 6. (i) DSTATCOM under constant loading, (ii) Harmonics spectrum of source current, (iii) Harmonics spectrum of load current and (iv) a-phase source voltage and source current waveform.

This difference is processed through the Proportional-Integral (PI) controller to manage the constant dc bus voltage. The output of PI controller can be expressed as

$$w_{dp} = k_{pdp} v_{de} + k_{idp} \int v_{de} dt \quad (17)$$

The sum of output of PI controller and the average magnitude of active component of load currents is the total active components of the reference source current can be expressed as

$$w_{spt} = w_{dp} + w_{lp} \quad (18)$$

2.3. Computation of reactive component of reference source currents

The difference in between reference ac voltage ' $v_{t(ref)}$ ' and sensed ac voltage ' $v_t$ ' is the error in ac voltage ( $v_{te}$ ) can be expressed as

$$v_{te} = v_{t(ref)} - v_t \quad (19)$$

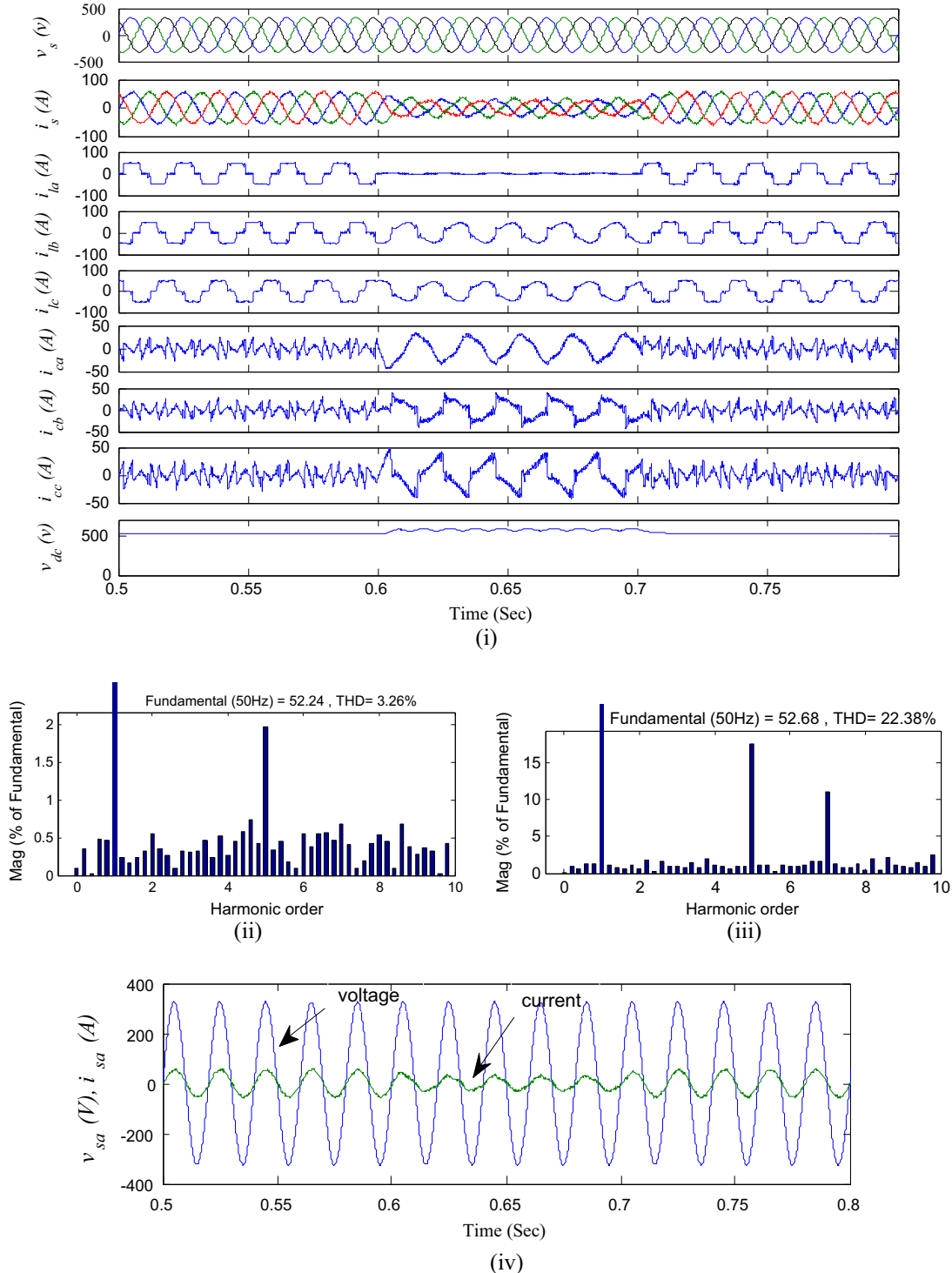


Figure 7. (i) DSTATCOM under variable loading, (ii) Harmonics spectrum of source current, (iii) Harmonics spectrum of load current and (iv) a-phase source voltage and source current waveform.



This difference is processed through the PI controller to manage the constant ac bus voltage. The output of PI controller can be expressed as

$$w_{qq} = k_{pq} v_{te} + k_{iq} \int v_{te} dt \quad (20)$$

The difference between output of PI controller and the average magnitude of reactive component of load current is the total reactive components of the reference source current can be expressed as

$$w_{sqt} = w_{qq} - w_{lq} \quad (21)$$

#### 2.4. Computation of switching signal generation

Three phase reference source active component are estimated by multiplying in phase unit voltage and active power current component of respective phase and these are obtained as

$$\begin{bmatrix} i_{sap} \\ i_{sbp} \\ i_{scp} \end{bmatrix} = w_{spt} \begin{bmatrix} u_{ap} \\ u_{bp} \\ u_{cp} \end{bmatrix} \quad (22)$$

Similarly, three phase reference source reactive component are estimated by multiplying quadrature unit voltage and reactive current component of respective phase and these are obtained as

$$\begin{bmatrix} i_{saq} \\ i_{sbq} \\ i_{scq} \end{bmatrix} = w_{sqt} \begin{bmatrix} u_{aq} \\ u_{bq} \\ u_{cq} \end{bmatrix} \quad (23)$$

The summation of active and reactive components of current is called as reference source currents and these are obtained as

$$\begin{bmatrix} i_{sa}^* \\ i_{sb}^* \\ i_{sc}^* \end{bmatrix} = \begin{bmatrix} i_{sap} \\ i_{sbp} \\ i_{scp} \end{bmatrix} + \begin{bmatrix} i_{saq} \\ i_{sbq} \\ i_{scq} \end{bmatrix} \quad (24)$$

The both actual source currents ( $i_{sa}, i_{sb}, i_{sc}$ ) and the reference source currents ( $i_{sa}^*, i_{sb}^*, i_{sc}^*$ ) of the respective phases are compared then current error signals are fed to a Hysteresis current controllers (HCC). Their outputs are used to drive the power devices affianced in VSC.

### 3. Simulation results & discussion

To analyse the performance of CGBP based  $icos\phi$  control technique and to compare with  $icos\phi$  control technique of DSTATCOM is developed in MATLAB/ Power system Simulink toolbox which is depicted below figures.

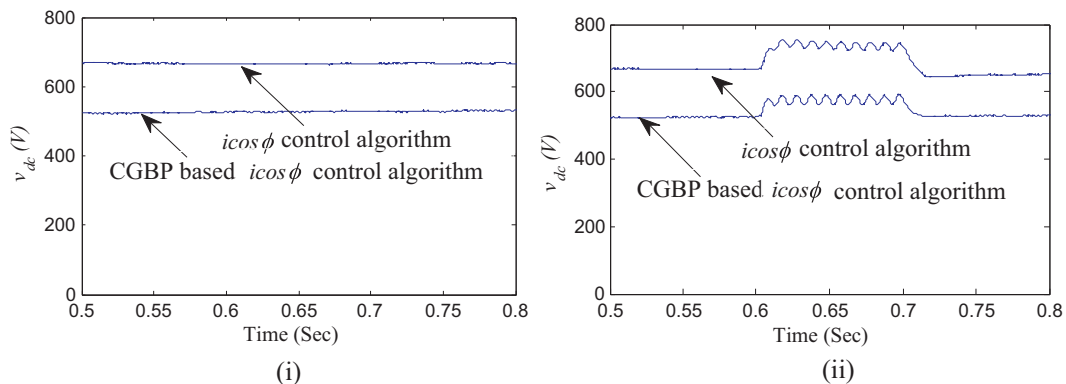


Figure 8. Comparative results under (i) constant loading and (ii) variable loading.

#### 3.1. DSTATCOM using $icos\phi$ control technique under balanced loading condition

The functional behaviour of distribution system including DSTATCOM using  $icos\phi$  control technique under balanced loading condition are shown in the Fig. 4(i)–(iv). Such condition is achieved, by putting load remains constant. The traces are capacitor voltage ( $v_{dc}$ ), compensating current ( $i_{ca}, i_{cb}, i_{cc}$ ), load current ( $i_{la}, i_{lb}, i_{lc}$ ), source current ( $i_s$ ) and source voltage ( $v_s$ ) organized from bottom to top in Fig. 4(i). The THD percentage of source and load current are 5.78 and 21.45 are shown in the Fig. 4(ii)–(iii) respectively. The a-phase source voltage and source current are showing the Power factor correction in Fig. 4(iv). The observation demonstrated that this technique performs source elimination, load balancing and voltage regulation but not so much satisfactory as per IEEE guidelines.

#### 3.2. DSTATCOM using $icos\phi$ control technique under unbalanced loading condition

The functional behaviour of distribution system including DSTATCOM using  $icos\phi$  control technique under unbalanced loading condition are shown in the Fig. 5(i)–(iv). Such condition is achieved, by releasing the load in a-phase from 0.6 s to 0.7 s. The traces are capacitor voltage ( $v_{dc}$ ), compensating current ( $i_{ca}, i_{cb}, i_{cc}$ ), load current ( $i_{la}, i_{lb}, i_{lc}$ ), source current ( $i_s$ ) and source voltage ( $v_s$ ) organized from bottom to top in Fig. 4(i). The THD percentage of source and load current are 5.85 and 21.89 are shown in Fig. 5 (ii)–(iii) respectively. The a-phase source voltage and source current are showing the Power factor correction in Fig. 5(iv). The observation demonstrated that this technique performs source elimination, load balancing and voltage regulation but not so much satisfactory as per IEEE guidelines.

#### 3.3. DSTATCOM using CGBP based $icos\phi$ control technique under balanced loading condition

The functional behaviour of distribution system including DSTATCOM using CGBP based  $icos\phi$  control technique under balanced loading condition are shown in Fig. 6(i)–(iv). Such condition is achieved, by putting load remains constant. The traces are capacitor voltage ( $v_{dc}$ ), compensating current ( $i_{ca}, i_{cb}, i_{cc}$ ), load current ( $i_{la}, i_{lb}, i_{lc}$ ), source current ( $i_s$ ) and source voltage ( $v_s$ ) organized from bottom to top in Fig. 6(i). The THD percentage of source and load current are 3.13 and 22.25 are shown in Fig. 6(ii)–(iii) respectively. The a-phase source voltage and source current are showing the Power factor correction in Fig. 6(iv). The observation demonstrated that this technique performs source elimination, load balancing and voltage regulation but not so much satisfactory as per IEEE guidelines.



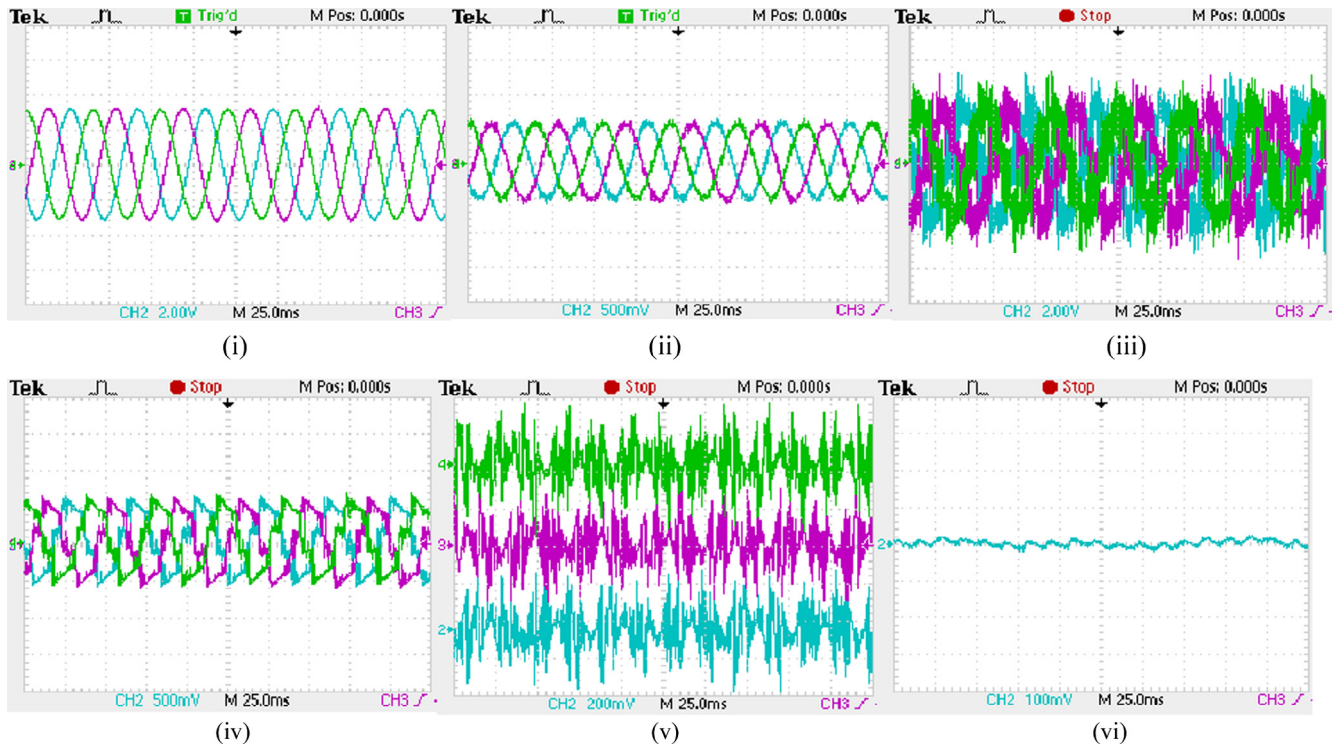


Figure 9. RTDS waveform for (i)  $v_s$ , (ii)  $i_s$ , (iii)  $v_h$ , (iv)  $i_h$ , (iv)  $i_c$  & (iv)  $v_{dc}$ .

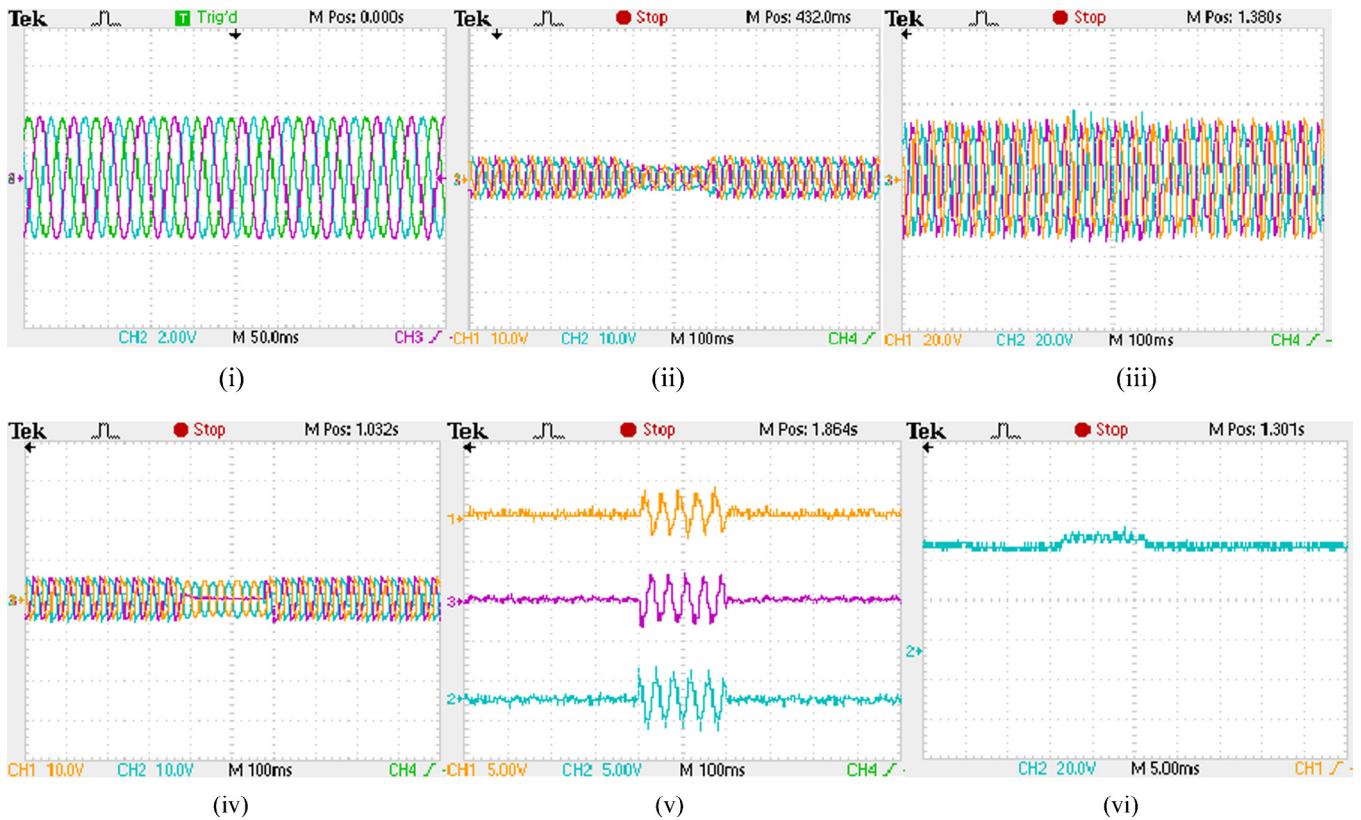


Figure 10. RTDS waveform for (i)  $v_s$ , (ii)  $i_s$ , (iii)  $v_h$ , (iv)  $i_h$ , (iv)  $i_c$  & (iv)  $v_{dc}$ .

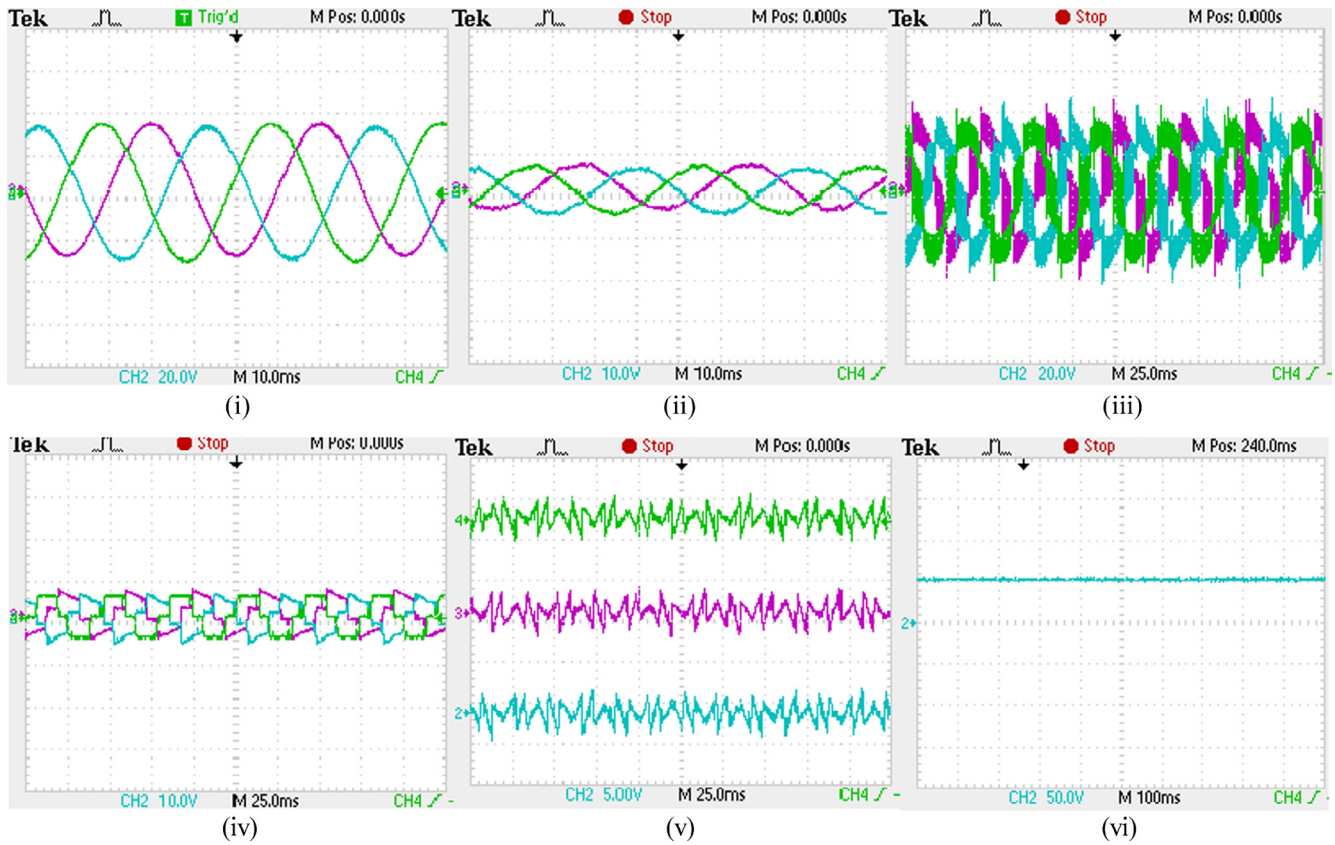


Figure 11. RTDS waveform for (i)  $v_s$ , (ii)  $i_s$ , (iii)  $v_h$ , (iv)  $i_c$  & (iv)  $v_{dc}$ .

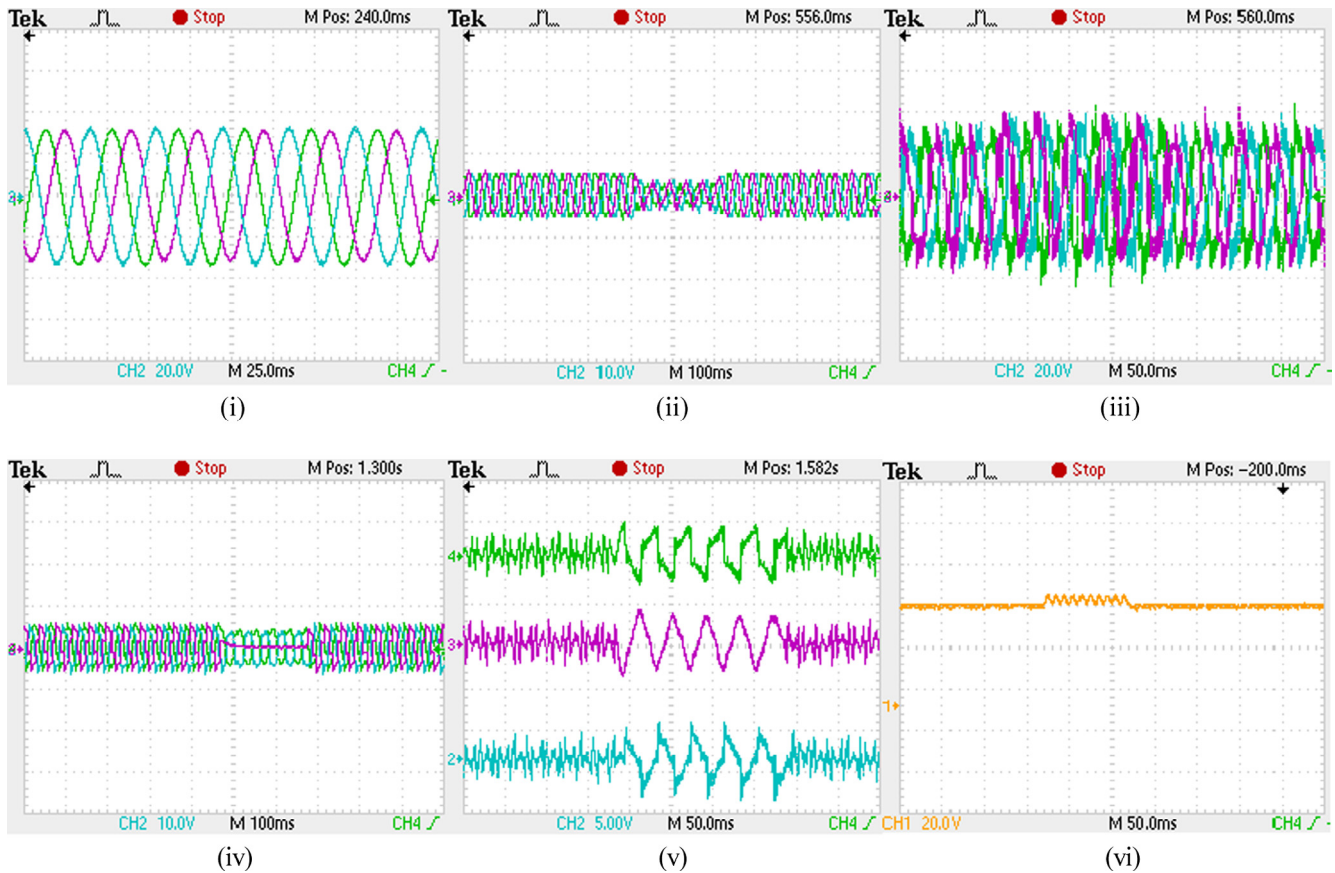


Figure 12. RTDS waveform for (i)  $v_s$ , (ii)  $i_s$ , (iii)  $v_h$ , (iv)  $i_c$  & (iv)  $v_{dc}$ .



### 3.4. DSTATCOM using CGBP based icos $\phi$ control technique under unbalanced loading condition

The functional behaviour of distribution system including DSTATCOM using CGBP based icos  $\phi$  control technique under unbalanced loading condition are shown in Fig. 7(i)–(iv). Such condition is achieved, by releasing the load in a-phase from 0.6 s to 0.7 s. The traces are capacitor voltage ( $v_{dc}$ ), compensating current ( $i_{ca}$ ,  $i_{cb}$ ,  $i_{cc}$ ), load current ( $i_{la}$ ,  $i_{lb}$ ,  $i_{lc}$ ), source current ( $i_s$ ) and source voltage ( $v_s$ ) organized from bottom to top in Fig. 7(i). The THD percentage of source and load current are 3.26 and 22.38 are shown in Fig. 7(ii)–(iii) respectively. The a-phase source voltage and source current are showing the Power factor correction in Fig. 7(iv). The observation demonstrated that this technique performs source elimination, load balancing and voltage regulation but not so much satisfactory as per IEEE guidelines. Current (iv) a-phase source voltage and source current waveform.

The more prominent comparison regarding the  $v_{dc}$  performance which is supporting to the voltage regulation of DSTATCOM are described below. Fig. 8(i) shows the performance of  $v_{dc}$  using both these algorithms under constant loading. In this figure, the value of  $v_{dc}$  is regulated at 661V by DSTATCOM using icos  $\phi$  algorithm while 535 V by DSTATCOM using CGBP based icos  $\phi$  control technique. Similarly, Fig. 8(ii) shows the performance of  $v_{dc}$  using both these algorithms under variable loading. In this figure, the value of  $v_{dc}$  is regulated at 720–754 V by DSTATCOM using icos  $\phi$  algorithm while 566–594 V by DSTATCOM using CGBP based icos  $\phi$  control technique in the interval of 0.6–0.7 s.

The following performance parameters are enumerated in table.

All the above discussion is in favour of CGBP based icos  $\phi$  control algorithm than other. So that, DSTATCOM using suggested algorithm will facilitate the better response in power quality issues for all possible of varying conditions.

## 4. RT-Lab simulation results

The performances between icos  $\phi$  control technique based DSTATCOM and CGBP controlled icos  $\phi$  technique based DSTATCOM are carried out. These analyses are obtained in a PC inbuilt with Opal RT-Lab software in real time [23,24]. The Opal RT-Lab simulation waveforms are obtained using digital storage oscilloscope (DSO) and these are presented in Figs. 9–12. The source current ( $i_s$ ), load current ( $i_l$ ), current ( $i_{ca}$ ,  $i_{cb}$ ,  $i_{ca}$ ) and dc-link voltage ( $v_{dc}$ ) for icos  $\phi$  control technique based DSTATCOM under various loading are depicted in Figs. 9(i–iv) and 10(i–iv) respectively. Similarly the above performance parameter for CGBP controlled icos  $\phi$  technique based DSTATCOM under various loading are depicted in Figs. 11(i–iv) and 12(i–iv) respectively. The scale 100A/div for  $i_s$ ,  $i_l$ ,  $i_c$  and 500 V/div for  $v_{dc}$  are used. The real time digital simulation results are in line with the simulation results and so confirm the superior performance of the CGBP controlled icos  $\phi$  technique based DSTATCOM. The various block parameters utilized for the purpose of simulation studies are shown illustrated in Appendix A.

## 5. Conclusion

A DSTATCOM using CGBP control technique is carried out in MATLAB/Simulink environment. The performance of this DSTATCOM is capable of achieving source current reduction, load balancing power factor correction and voltage regulation as per norms & regulation followed by IEEE-519 standard and more desirable in reducing the size of DSTATCOM and hence, it can be provide better economical solution for power quality problems with effectively and efficiently. One can be concluded in nominating the particular topology with such control algorithm for DSTATCOM. It can be

hoped that this research work will significant impact on user, designer, manufacturer, researcher & power engineer for further correction of power quality.

## Appendix A

Three phase supply voltage 230 V (L – L), 50 Hz, Source resistor:  $R_s = 0.04 \Omega$ , Source inductor:  $L_s = 0.04$  mH, 3P3W full bridge uncontrolled rectifier with  $R = 13 \Omega$ ,  $L = 200$  mH,  $v_{dc(ref)} = 700$  V,  $v_{t(ref)} = 325$  V,  $L_f = 1.5$  mH,  $R_s = 0.04 \Omega$ ,  $w_0 = 0.4$ ,  $w_{01} = 0.2$ ,  $\mu = 0.6$ ,  $k_1 = 0.4$ ,  $k_2 = 0.1$ , cut of frequency of LPF in the dc bus controller = 10 Hz, cut of frequency of LPF in the ac bus controller = 10 Hz, PI controller gain in the dc side  $k_{pdp} = 2$ ,  $k_{idp} = 3.5$  and dc link capacitor = 2000  $\mu$ F, etc.

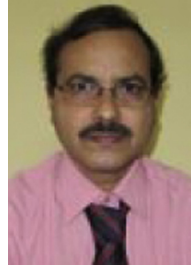
## References

- [1] Moreno-Munoz A. Power quality: mitigation technologies in a distributed environment. London Limited: Springer-Verlag; 2007.
- [2] Bollen Math H. Overview of power quality and power quality standards. Understanding power quality problems: voltage sags and interruptions, vol. 1. Wiley-IEEE Press; 2000.
- [3] Singh Bhim, Jayaprakash P, Kothari DP. New control approach for capacitor supported DSTATCOM in three-phase four wire distribution system under non-ideal supply voltage conditions based on synchronous reference frame theory. Int J Electr Power Energy Syst 2011;35(5):1109–17.
- [4] Chauhan SK, Shah MC, Tiwari RR, Tekwani PN. Analysis, design and digital implementation of a shunt active power filter with different schemes of reference current generation. IET Power Electron 2014;7(3):627–39.
- [5] Montero M, Cadaval E, Gonzalez F. Comparison of control strategies for shunt active filter in three-phase four-wire systems. IEEE Trans Power Electron 2007;22(1):229–36.
- [6] Rahmani Salem, Hamadi Abdel Hamid, Kamal Al-Haddad. A Lyapunov-function-based control for a three-phase Shunt hybrid active filter. IEEE Trans Ind Electron 2012;59(3):1418–29.
- [7] Wang H, Li Q, Wu M. Investigation on a new algorithm for instantaneous reactive and harmonic currents detection applied to intensive nonlinear loads. IEEE Trans Power Deliv 2007;22(4):2312–8.
- [8] Ghosh A, Joshi A. A new approach to load balancing and power factor correction in power distribution system. IEEE Trans Power Deliv 2000;15(1):417–22.
- [9] Kabir MA, Mahub U. Synchronous detection and digital control of shunt active power filter in power quality improvement. In: Power energy conf Illinois (PECI), p. 1–5.
- [10] Singh BN. Design and digital implementation of active filter with power balance theory. IEEE Proc Electr Power Appl 2005;152(5):1149–60.
- [11] Kannan V, Kamatchi, Rengarajan N. Investigating the performance of photovoltaic based DSTATCOM using icos  $\phi$  algorithm. Int J Electr Power Energy Syst 2014;54:376–86.
- [12] Bhubaneswari G, Nair MG. Design, simulation and analog circuit implementation of a three phase shunt active filter using icos  $\phi$  algorithm. IEEE Trans Power Deliv 2008;23(2):1222–35.
- [13] Badoni M, Singh A, Singh B. Adaptive neurofuzzy inference system least-mean-square-based control algorithm for DSTATCOM. IEEE Trans Ind Inf 2016;12(2):483–92.
- [14] Rigatos Gerasimos G. Advanced model of neural networks. Berlin Heidelberg: Springer-Verlag; 2015.
- [15] Kumar P, Mahajan A. Soft computing techniques for the control of an active power filter. IEEE Trans Power Deliv 2009;24(1):452–61.
- [16] Singh B, Arya SR. Back-propagation control algorithm for power quality improvement using DSTATCOM. IEEE Trans Ind Electron 2014;61(3):1204–12.
- [17] Jayachandran J, Sachithanandam R Murali. Neural network-based control algorithm for DSTATCOM under nonideal source voltage and varying load conditions. Can J Electr Comput Eng 2015;38(4):307–17.
- [18] Anbazhagan S, Kumarappan N. Day-ahead deregulated electricity market price forecasting using recurrent neural network. IEEE Syst J 2013;7(4):866–72.
- [19] Qin S, Xue X. A two-layer recurrent neural network for nonsmooth convex optimization problems. IEEE Trans Neural Netw Learn Syst 2015;26(6):1149–60.
- [20] Xiao L, Zhang Y. Zhang neural network versus gradient neural network for solving time-varying linear inequalities. IEEE Trans Neural Netw 2011;22(10):1676–84.
- [21] Xia Y, Wang J. A bi-projection neural network for solving constrained quadratic optimization problems. IEEE Trans Neural Netw Learn Syst 2016;27(2):214–24.
- [22] Saini L Mohan, Soni M Kumar. Artificial neural network-based peak load forecasting using conjugate gradient methods. IEEE Trans Power Syst 2002;17(3):907–12.
- [23] RT-Lab Professional. <http://www.opal-rt.com/product/rt-lab-professional>.

- [24] Panda AK, Patnaik SS. Analysis of cascaded multilevel inverters for active harmonic filtering in distribution networks. *Int J Electr Power Energy Syst* 2015;66:216–26.



**Mrutyunjaya Mangaraj** received the B.Tech in Electrical Engineering from Berhampur University, India in 2006. He received the M.Tech in Power System Engineering from VSSUT, Burla, India in 2010. He served as Assistant professor in the Department of Electrical Engineering at NIST Berhampur, India from 2010 to 2013 and currently pursuing Ph.D. in National Institute of Technology, Rourkela since 2014 onwards. His area of research interest includes Power System Economics, Design and modelling of d-FACTS devices with Embedded Controller, Soft computing techniques etc.



**Anup Kumar Panda** received the B.Tech in Electrical Engineering from Sambalpur University, India in 1987. He received the M.Tech in Power Electronics and Drives from Indian Institute of Technology, Kharagpur, India in 1993 and Ph.D. in 2001 from Utkal University. Join as a faculty in IGIT, Sarang in 1990. Served there for eleven years and then join National Institute of Technology, Rourkela in January 2001 as an assistant professor and currently continuing as a Professor in the Department of Electrical Engineering. He has published over hundred articles in journals and conferences. He has completed two MHRD projects and one NaMPET project. Guided six

Ph.D. scholars and currently guiding six scholars in the area of Power Electronics & Drives. His research interest include analysis and design of high frequency power conversion circuits, power factor correction circuits, power quality improvement in power system and electric drives, Applications of Soft Computing Techniques.